Journal of Hydrology 452–453 (2012) 25–39

Contents lists available at SciVerse ScienceDirect

Journal of Hydrology

journal homepage: www.elsevier.com/locate/jhydrol

Assessment of mineral concentration impacts from pumped stormwater on an Everglades Wetland, Florida, USA – Using a spatially-explicit model

Chunfang Chen [a,*], Ehab Meselhe [a], Michael Waldon [b]

[a] Center for Louisiana Waters Studies, Institute of Coastal Ecology and Engineering, University of Louisiana at Lafayette, P.O. Box 42291, Lafayette, LA 70504, United States
[b] Everglades Program Team, A.R.M. Loxahatchee National Wildlife Refuge, 10216 Lee Rd., Boynton Beach, FL 33473, United States

ARTICLE INFO

Article history:
Received 2 September 2011
Received in revised form 7 May 2012
Accepted 8 May 2012
Available online 23 May 2012
This manuscript was handled by Geoff Syme Baveye, Editor-in-Chief

Keywords:
Spatially explicit model
Everglades
Wetland hydrodynamics
Constituent transport
Impact analysis
MIKE FLOOD

SUMMARY

The Arthur R. Marshall Loxahatchee National Wildlife Refuge (Refuge) overlays a 58,725 ha remnant of the Northern Everglades which is termed Water Conservation Area 1 (WCA-1). The Refuge is impacted by stormwater inflow from flood control pump stations which discharge to a perimeter canal system inside an impounding levee. These discharges contain elevated mineral and nutrient concentrations, with chloride concentration averaging well over 100 mg/L. It has long been established that the Refuge naturally has low mineral content softwater, and that this low-mineral condition affects the species composition of wetland periphyton that are at the base of much of the Refuge food chain. The interior marsh of the Refuge has today been termed rainfall-driven or ombrotrophic, with median chloride concentration averaging 20.5 mg/L. However, chloride concentration in rain water averages roughly 2 mg/L. The level of impact of exogenous pumped inflow on the concentration of chloride and other mineral constituents in the interior marsh has been unclear, and at times it has been debated whether atmospheric loading and evaporation can alone explain observed concentration of chloride in the interior. We applied a spatially explicit hydrodynamic and constituent transport model, MIKE FLOOD, to estimate the unimpacted condition of the interior. We compare this with simulated and monitored chloride concentrations under current conditions. The model was calibrated for a 5-year period (2000–2004), and validated for a 2-year period (2005–2006). We found that when pumped inflow concentration is reduced to an estimated rainfall chloride concentration, interior chloride concentration ranges typically below 5 mg/L. We therefore conclude that the interior chloride concentration is currently dominated by pumped inflows and should not be termed ombrotrophic. We also present initial modeling of one proposed remedial solution for reducing this impact. Our study demonstrates the feasibility and utility of modeling constituent concentrations in large wetlands that are flooded by overbank flow from streams or canals. This model quantifies the importance of surface water transport mechanisms across the Refuge linking wetland concentration to inflow concentration and volume.

1. Introduction

An ombrotrophic wetland receives all its water and nutrients from the atmosphere, and is therefore acidic and low in nutrients and minerals (Charman, 2002). Within the modern Everglades wetlands, this status is uniquely attributed to the Arthur R. Marshall Loxahatchee National Wildlife Refuge (Refuge). This attribution is based on the observed steep spatial gradient of mineral concentration in surface water near the perimeter canal, and the relatively low and uniform concentrations measured at most-interior and least-impacted sampling sites (Browder et al., 1991, 1994; Swift, 1981, 1984; Swift and Nicholas, 1987). Here, we use a spatially-explicit hydrologic and transport model, MIKE FLOOD, to assess the degree to which the Refuge interior mineral content is impacted by surface water inflows, and to determine if a classification of ombrotrophic is appropriate.

The Refuge (Fig. 1) overlays Water Conservation Area 1 (WCA-1), and is managed by the United States Fish and Wildlife Service (USFWS). WCA-1 is a 587 km^2 remnant of the Northern Everglades in Palm Beach County, Florida (USFWS, 2000). Wetland loss and degradation has taken place in the greater Everglades. The USFWS recognized that there have been changes to the Refuge's water quantity, timing, and quality which have caused negative impacts to the Refuge's ecosystem. The Refuge is impacted by changes in water flow and stage (Brandt et al., 2000; USFWS, 2000; Brandt, 2006), excessive nutrient loading (Newman et al., 1997; USFWS, 2000), and altered dissolved mineral concentrations including chloride (Swift, 1981, 1984; Swift and Nicholas, 1987; Browder

* Corresponding author. Tel.: +1 337 482 6847.
E-mail address: chunfang.chen0@gmail.com (C. Chen).

0022-1694/$ - see front matter © 2012 Elsevier B.V. All rights reserved.
http://dx.doi.org/10.1016/j.jhydrol.2012.05.016

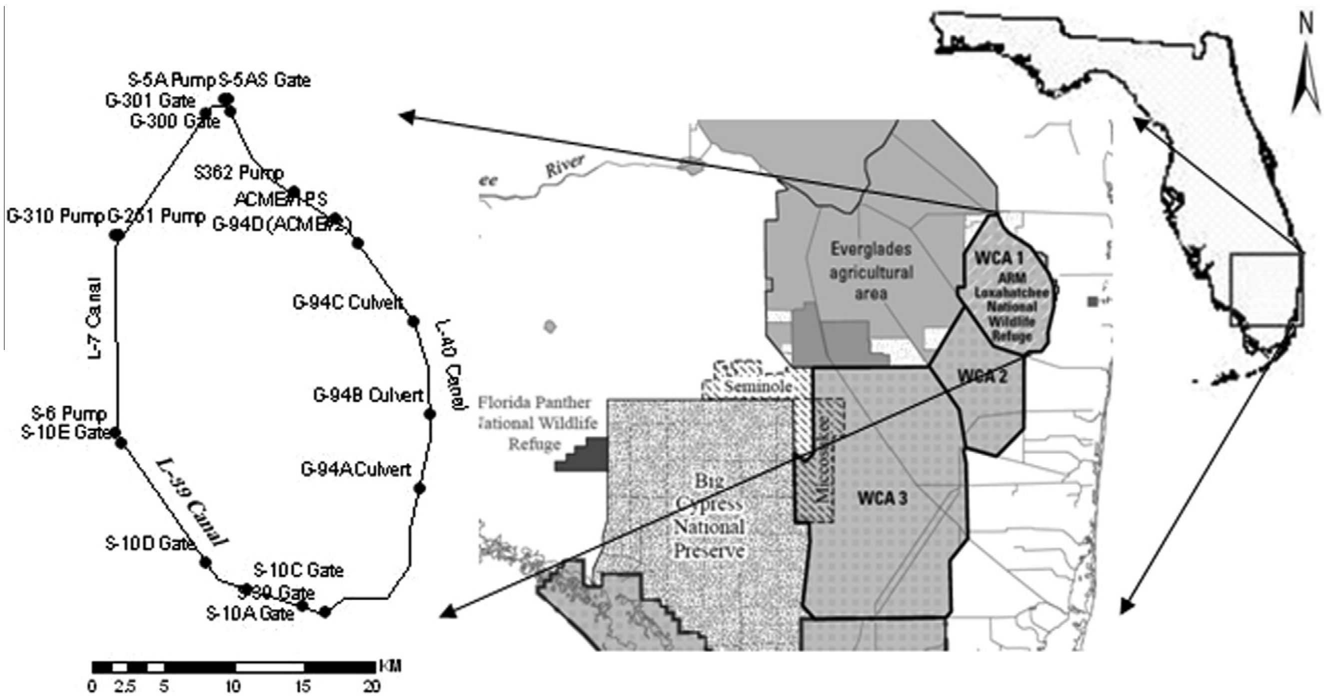

Fig. 1. Boundaries of the Loxahatchee Refuge and locations of the hydraulic structures in the canal (modified from U.S. Fish and Wildlife Service, 2000).

et al., 1991, 1994; McCormick and Crawford, 2006). The Refuge has supported development of hydrodynamic and water quality models to gain a better understanding of these impacts and to evaluate alternative water management options that may reduce these impacts.

The ability to predict the effects of manipulation of water operations upon wetlands is central to the success of wetland management and restoration (Gilvear and Bradley, 2000; Hollis and Thompson, 1998). Hydrodynamic and water quality models provide the predictive tool needed for management and scientific support. A calibrated hydrodynamic and water quality model provides managers and planners with information on movement of water, and the fate and transport of constituents (Kadlec and Hammer, 1988; Tsanis et al., 1998; Koskiaho, 2003). Models provide a tool to assist in answering questions regarding the hydrologic, hydrodynamic, and water quality conditions occurring under present conditions and management rules, and models project how these processes would be altered by alternative structural changes and management scenarios.

Other Refuge modeling studies have utilized spatially aggregated designs (Arceneaux et al., 2007; Wang et al., 2008, 2009; Roth, 2009; Meselhe et al., 2010). However, such models are less appropriate for site-specific applications or where detailed spatial analysis and visualization is needed. Therefore, efforts reported here have been directed towards development of a distributed physically based model (Martin and Reddy, 1991; Alvord and Kadlec, 1996). In addition, for model calibration, previous hydrological models of the Refuge used historical flow records to define not only the inflow, but also the outflow boundary (SFWMD, 2005a). Using only historic outflow for calibration does not provide a test of the rule-based outflow management that is necessary when testing scenarios that do not apply the historic inflow time series. In this study, we simulate regulatory outflows based on predefined stage–discharge relationship. In modeling the hydrodynamics and chloride concentration in the Refuge, a spatially explicit model was developed using MIKE FLOOD (Danish Hydraulic Institute, DHI, 2008; Chen et al., 2010) to provide a detailed quantitative framework. This paper describes the model development, calibration, validation, and then documents model results which assess impact of pumped inflows on wetland mineral status.

2. Study area

2.1. Site description

The Refuge is located 11.3 km west of the city of Boynton Beach, Florida in the southeastern United States (Fig. 1). It is enclosed within a levee system and a perimeter canal along the interior of the levee (Richardson et al., 1990). The Refuge landscape consists of a complex mosaic of wetland communities that grade from wetter sloughs and wet prairies, to sawgrass, brush, and finally tree islands occurring at the dryer end of the scale (USFWS, 2000). Refuge water conditions are controlled by the inflows and outflows through pumps and gates along the perimeter canal. Land use in areas bordering the Refuge varies from drained agricultural land (the Everglades Agricultural Area) on the northwest boundary, urban development to the east, and Everglades wetlands of Water Conservation Area 2A (WCA-2A) located southwest of the Refuge.

Refuge topography is characterized by a fairly flat interior marsh (Fig. 2) and a varying-section perimeter canal. The marsh elevation data were collected by the United States Geological Survey (USGS) on a 400 by 400 m grid (Desmond, 2003). Elevation ranges from 5.64 to 3.23 m (NGVD29) decreasing slightly from north to south which, at times, may cause a slow southward surface water flow (Meselhe et al., 2005). Perimeter canal cross-section elevation data were collected by the University of Florida's Institute of Food and Agricultural Sciences with approximate 1600 m resolution (Daroub et al., 2002) and was supplemented by measurements taken by the USFWS. The sediment surface elevation for the eastern canal (L-40) and the western canals (L-7 and L-39) vary with a mean elevation of 0.98 and 0.73 m, respectively (Meselhe et al., 2005).

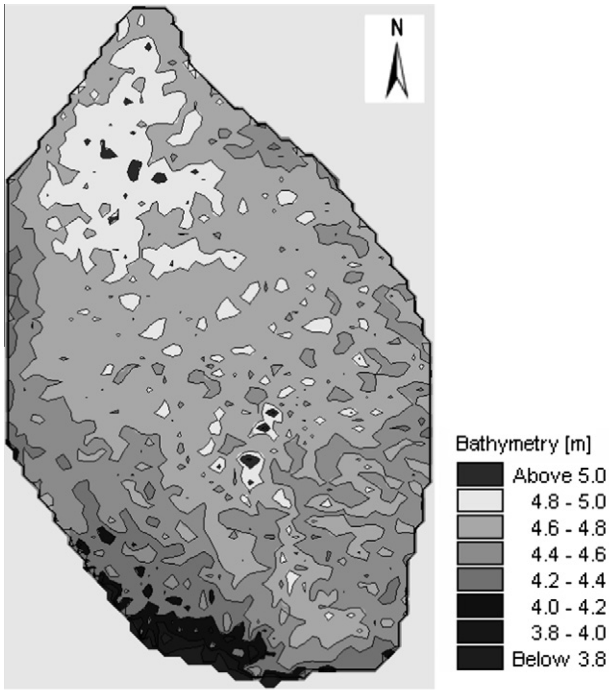

Fig. 2. Topography of the Refuge (in m NGVD 1929) based on USGS published elevations. Desmond (2003).

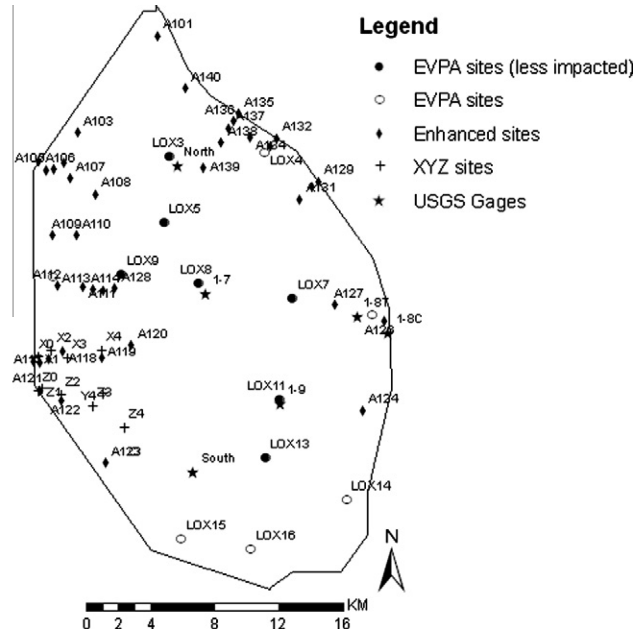

Fig. 3. Water level and water quality monitoring sites located in the Refuge (enhanced stations, labeled LOXA elsewhere, are labeled A here for brevity). Here 7 marsh stations denoted (LOX3, LOX5, LOX7, LOX8, LOX9, LOX11, and LOX13) were conjectured to be least impacted by the canal inflow.

Water and nutrients enter and exit the Refuge through 19 hydraulic structures located around the perimeter canal (Fig. 1). Water is pumped from inflow pump stations into the Refuge. Several structures are bidirectional. The major outflow structures (S-10A, S-10C, S-10D, and S39) are located toward the southern end of the Refuge. Historical flow records for these structures are maintained by the South Florida Water Management District (SFWMD) in a publicly-available online database, DBHYDRO (http://www.sfwmd.gov/dbhydroplsql/show_dbkey_info.main_menu).

2.2. Water regulation schedule

Excessive water levels in the Refuge are reduced to meet stage limits through mandatory discharges out of the Refuge (regulatory releases) under a seasonally varying regulation schedule. The Refuge water regulation schedule (WRS) is administered by the U.S. Army Corps of Engineers (USACE, 1994), Jacksonville District in consultation with other agencies (Arceneaux et al., 2007). The WRS has sets stage limits (floor) that vary from 4.8 m at the end of the dry season, up to 5.33 m at the end of the wet season. When stage is above this limit, the WRS is said to be in Zone A1, and release of water is mandatory.

2.3. Field data

The daily-averaged structural flows were obtained from DBHYDRO. Daily total precipitation and evapotranspiration data from available gages were acquired from various sources (Meselhe et al., 2005). Five continuous water level stations maintained by USGS are located in the marsh, and another station (1-8C) is located in the eastern canal (L-40) (Fig. 3). Water depth, termed Depth to Consolidated Substrate (DCS), was measured by the USFWS (2007) when marsh water quality samples were collected monthly at marsh stations (Fig. 3). Chloride concentration measured from grab samples were obtained from five data collection programs: (1) the Everglades Protection Area Project (EVPA) water quality stations; (2) enhanced water quality monitoring stations (data available after August 2004, alternatively termed LOXA or A stations); (3) SFWMD transect monitoring sites (also known as the XYZ sites); (4) water quality monitoring sites located at the structures; and (5) additional independent monitoring sites (Meselhe et al., 2005).

3. Methods

3.1. Modeling framework

MIKE FLOOD is a spatially distributed and physically based modeling environment. It integrates a 1-dimensional channel model (MIKE 11) with the grid of a 2-dimensional surface flow model (MIKE 21) through user-defined couplings at the interfaces. After each computational time step, the computed data are exchanged between the two models. The hydrodynamic (HD) module in MIKE 21 solves the unsteady depth-integrated 2-dimensional continuity and momentum equations using the Alternating Direction Implicit (ADI) technique. The HD module in MIKE 11 solves the fully dynamic Saint Venant equations using the 6-point Abbot Finite Difference Scheme. Water constituent transport in MIKE 21 and MIKE 11 are simulated by the Advection–Dispersion (AD) modules, which use velocity from the HD module to solve the advection–dispersion equation. The open-source ECO Lab module is used to define the mass balance relationship including the reactive and settling process for water constituent in MIKE 21. MIKE 11 also simulates a broad range of hydraulic structures including weir, gate, bridge, culvert, and control structure. Details about MIKE FLOOD can be found in the Reference Manual (2008 Ed.). Note that the singular use of "model" refers to the coupled MIKE 11 and MIKE 21 model.

3.2. Calibration–validation analysis

The ability of the model to reproduce observed stage, depth, and chloride concentration was quantified for calibration and validation periods using statistical measures (Chen et al., 2010). The model residual is the model prediction minus the observed value. Bias is the average residual and is a measure of under- or over-prediction. Root mean square error, RMSE, is the square root of the average of the squared residuals, representing the "typical" or "average" error to be expected (Berry and Lindgren, 1996). Variance reduction is equal to one minus the residual variance divided by the variance of the observed values, and represents how well the model output data follow the variations in the observed data. The sample correlation coefficient, r, estimates the covariance of the observed and modeled values divided by the product of their standard deviations, and is a dimensionless representation of the linear relationship between the observed and modeled data. Nash–Sutcliffe efficiency (Nash and Sutcliffe, 1970), reflecting both the bias and the variance reduction, can vary from an unboundedly large negative value to positive one for a perfect fit, and is widely applied to measure overall reliability of model projection. A value of 0 indicates the model and the average value of the observed data are equal in their ability as predictors.

4. Model setup and inputs

4.1. Marsh model

The 2-dimensional MIKE 21 model domain represents the Refuge marsh with a uniform Cartesian grid of 400 m resolution which is compatible with available USGS topographic data (Desmond, 2003). Spatial rainfall was generated from measured data at available rainfall stations using inverse-distance weighting. As the measured potential ET was taken from a single station adjacent to the Refuge, and marsh sites that go dry for even a few weeks have considerably lower annual ET loss, the measured ET was adjusted when observed water depth was low by a reduction factor of f_{ET} (Arceneaux et al., 2007; Meselhe et al., 2010):

$$ET_{act} = f_{ET} * ET_{obs} \tag{1}$$

$$f_{ET} = \max\left(f_{ET\min}, \min\left(1, \frac{H}{H_{ET}}\right)\right) \tag{2}$$

where ET_{act} is the actual ET estimated from ET reduction (mm/d); ET_{obs} the measured potential ET (mm/d); $f_{ET\min}$ the minimum reduction of ET due to shallow water depth (%); H the estimated water depth (m) and H_{ET} is the depth above which ET is not reduced (m)$f_{ET\min}$ and H_{ET} are determined via calibration. Eq. (2) shows that f_{ET} depends on the water depth at specific location. To obtain spatially varied daily ET, interpolation was performed to the daily observed water level on each grid and transformed to the corresponding water depth (H). Then the water depth (H) was substituted into Eq. (2) to compute f_{ET}, which then is plugged in Eq. (1) to calculate ET_{act}.

Although groundwater model was not included, groundwater seepage was considered, which was assumed constant and uniformly distributed across the marsh. The vegetation was classified into six categories defined by the SFWMD (2000), and followed the vegetation mapping of Richardson et al. (1990) from 1987 imagery: sawgrass, cattail, open water and sloughs, wet prairie, tree island, and brush. The resistance for each grid was derived in GIS from vegetative class and expressed in Manning's M ($m^{1/3}$/s), the reciprocal of Manning's n (Table 1).

The drying and rewetting processes of the marsh were accounted for by the dry and wet depths. Velocity based Smagorinsky formula (DHI Water and Environment, 2008) was selected for turbulence with the Smagorinsky constant set to 0.5.

Chloride was modeled as a conservative tracer. The current induced transport was simulated by the AD module. The external factors, such as rainfall, transpiration, seepage, and aerial deposition were simulated using the template that the ECO Lab interface provides. Transpiration was assumed to carry constituent into the ground, and was defined using a single constant fraction of ET (Zhang et al., 2002; Andersen et al., 2001; Arceneaux et al., 2007) which was determined via calibration. Concentrically distributed temporally constant dispersion coefficients in six levels were defined, which gradually increases from the peripheral zones towards the interior. Wet and dry depositions were assumed to be spatially uniform and temporally constant. The initial water level in the marsh was estimated using the average of the observations at marsh stations. The spatially varied initial concentration was generated from the observed concentration of interior stations. A time step of 5 min was adequate for simulating hydrodynamics only. For the AD module, a reduced time step of 3 min was required to maintain stability.

Table 1
Manning's n for the six vegetation categories.

Vegetation type	Manning's n (s/$m^{1/3}$)
Sawgrass	4
Cattail	4
Open water and sloughs	0.8
Wet prairie	4
Tree island	2
Brush	2

4.2. Canal model

Available cross-sectional data were used to define the perimeter canal. Observed inflow and discrete chloride concentrations from grab samples were imposed at the inflow boundary structures. The regulatory discharges through the structures of S-10A, S-10C, S-10D, and S-39 were defined as a function of the difference in stage between station 1-8C and the WRS zone A1 floor. The discharge-stage difference relationship for the S-10 structures (S-10A, S-10C and S-10D) was derived based on the observed stage and outflow from January 1995 to August 2007. The regulatory discharge for S-39 was estimated using the ratio of the historical regulatory release of S-39 to that of the S-10 structures. The regulated release was modeled via MIKE 11 control structure. For water supply discharge and all non-regulatory structural releases, historical data were imposed at the boundaries.

Spatially uniform and temporally variable precipitation and evaporation were applied for the canal. Seepage from the canal was assumed constant in time and uniform in space, and was simulated as a boundary outflow that was determined via calibration. Manning's equation was used to simulate channel resistance, for which uniform Manning's n was assumed and calibrated. Canal dispersion was modeled using the exponential function

$$D = aV^b \tag{3}$$

where V is the velocity, a and b are calibration parameters. The wet and dry chloride depositions applied for the marsh were also adopted for the canal. The initial canal stage was estimated by the observed water level at 1-8C. The average observed concentration at canal stations was used for the initial concentration. The same time step used in MIKE 21 was applied in MIKE 11.

4.3. Coupled model

The model was initially setup to laterally couple the reaches of the MIKE 11 with the adjacent MIKE 21 cells. However, tests revealed that lateral link performs well in preserving mass for hydrodynamics, but has significant mass conservation error for the AD module. To resolve this problem, standard link was used, in which short channels were created which connect the perimeter channels of MIKE 11 and the adjacent fringe marsh cells in MIKE 21.

5. Model calibration and validation

A 5-year period (2000–2004) was selected for calibrating the model (Table 2). This period contains both high and low flow years, and is helpful to evaluate the model's capability to capture the variation of hydro-pattern. The 2-year period of 2005–2006 was selected for model validation. The model was manually calibrated through "trial and error" for hydrodynamics first and then for chloride concentration. The fine tuning of parameters was restricted to a physically-realistic range. Model performance in the calibration and validation process was evaluated both qualitatively, based on graphical visualization, and quantitatively, based on statistical measures.

The calibration parameters for hydrodynamics for MIKE 21 include resistance and seepage, dry and wet depths, minimum ET reduction $f_{ET\mathrm{min}}$, and minimum depth for ET reduction H_{ET} (Eq. (2)). Those for MIKE 11 include resistance and seepage. Preliminary results showed that stage was insensitive to roughness, especially for the canal. Stage was found to be sensitive to the total seepage, but insensitive to the ratio between the marsh and the canal. A series of values for the dry depth were tested ranging from 0.01 m to 0.05 m. The wet depth was examined over the range from 0.012 m to 0.1 m. These two parameters showed insignificant influence to stage. For $f_{ET\mathrm{min}}$ and H_{ET}, several sets were calibrated to encompass the physical limits for each. Calibration results varying these ET parameters indicated that different combinations give similar predictions; thus, this parameter set is not uniquely defined through stage calibration.

The calibration parameters for AD module in MIKE 21 and MIKE 11 include aerial (wet and dry) depositions, seepage, and dispersion. The transpiration fraction of ET in the marsh was another calibration parameter for MIKE 21. The wet and dry depositions calibrated from a companion study (Arceneaux et al., 2007) provided good results, and were adopted in this model. The total seepage calibrated from the hydrodynamic model was further split and assigned to the marsh and the canal. The six levels of dispersion coefficient defined for the marsh were calibrated. For the dispersion in the canal, a uniform and constant coefficient was assumed (i.e., $b = 0$ in Eq. (3)).

Chloride concentration was found to be highly sensitive to marsh transpiration. The calibrated transpiration fraction of ET was 35%. The overall chloride mass balance demonstrated to be sensitive to the seepage ratio between the marsh and the canal. This could be attributed to the fact that the typical canal concentration is much higher than that of the marsh, thus the canal seepage transports more chloride per unit flow than the marsh seepage. The final calibrated ratio of marsh and canal seepage is 1:1. The six levels of dispersion coefficient were assigned to the fringe towards the interior marsh. The calibrated values were 0.001, 0.3, 0.5, 0.8, 1.5, and 2.0 m^2/s. These values fall within the range given by Kadlec and Knight (1996). In calibrating the dispersion coefficients, numerical dispersion was considered, especially for the fringe marsh, which led to the relatively large gradient between the two outer most levels. Chloride transport in the canal is dominated by advection and chloride concentration showed only slight variation to changes in canal the canal dispersion coefficient. The final calibrated canal dispersion was 50 m^2/s, which is not atypical for natural channels (Bowie et al., 1985).

Two other parameters of dry and wet depths and the marsh roughness, which were previously found to have only minor impacts on predicted stage during the calibration for hydrodynamics, demonstrated significant impact on predicted chloride concentration. This difference in parametric sensitivity supported a more reliable and robust hydrodynamic model calibration. The dry and wet depths were identified through chloride calibration to be 0.050 and 0.052 m, respectively. Early stage calibration attempts over-predicted chloride concentration in the western marsh near the S-6 pump station. It was conjectured that this anomaly is caused by the limitation of the 1987 imagery (Richardson et al., 1990) to capture recent vegetation change in this area. Vegetation in this area was re-evaluated by inspecting the images from Google Earth (http://earth.google.com). We found an enlarged strip of dense vegetation along the perimeter canal in the southwestern Refuge which was consistent with anecdotal field observations of dense cattails invading areas surrounding water quality sampling sites in this area. Model vegetative resistance was thus adjusted accordingly.

6. Calibration and validation results

Graphical and statistical results of model calibration and validation are presented in this section. Additional details regarding the model results can be found in Chen et al. (2010).

6.1. Stage and depth

The model agreed well with observed water levels, captured the overall trends and seasonal variations, and had calibration errors of reasonable magnitude (Fig. 4, Tables 3 and 4). It is recognized that the point measurements at monitoring stations limit model evaluation to a simple comparison of modeled and observed at the gages. Although the model grid of 400 m resolution applied was based on the best available Refuge topographic data, smaller scale topographic (microtopographic) features were not included that likely have significant influence on site-specific stage, water depth,

Table 2
Calibrated hydrodynamic and chloride model parameters.

	Parameters	Unit	Value
Marsh	Roughness	$m^{1/3}/s$	0.125–1.25 (spatial variable)
	Seepage	m^3/s	2.25 (spatially uniform)
	Dry/wet depth	m	0.050/0.052
	Depth reduction factor	none	0.2
	Depth reduction boundary	m	0.2
	ET percent as transpiration	%	35
	Dispersion	m^2/s	0.001–2 (six concentric zones)
Canal	Roughness	$s/m^{1/3}$	0.03
	Seepage	m^3/s	2.25 (spatially uniform)
	Dispersion	m^2/s	50
Marsh and Canal	Chloride wet deposition	mg/L	2
	Chloride dry deposition	mg/m^2 yr	500

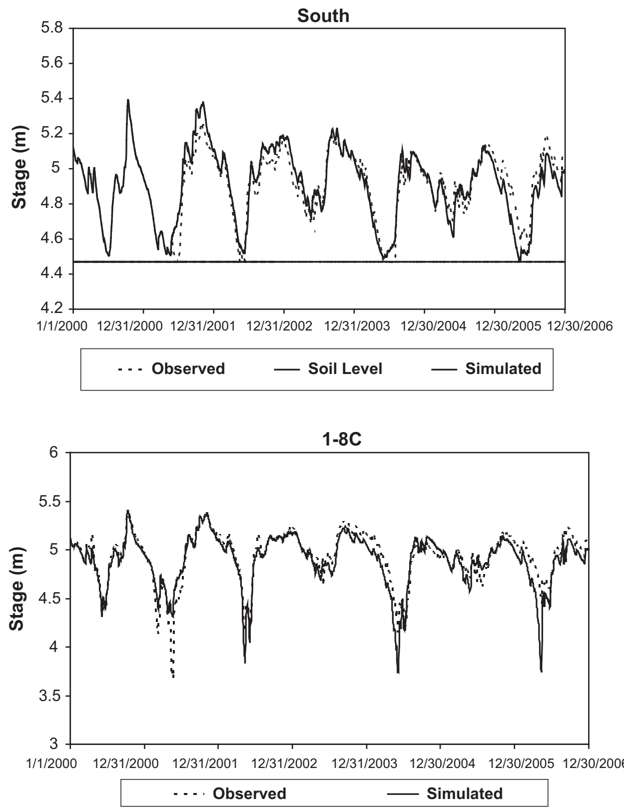

Fig. 4. Comparisons of modeled and observed water level at selected marsh and canal stations.

flow, and constituent concentrations. Discrepancies between simulated and observed stage are largely attributed to uncertainty in model inputs, such as temporal aggregation in daily averaged flows and precipitation. The model is not expected to capture stage response to events of time scale smaller than daily. This is more apparent for low stage events, such as the dry period during May 2001 in the canal when small diel fluctuation in canal stage was observed. Uncertainty in ET estimation also likely contributes significantly to calibration error because only one ET station located to the northwest of the Refuge is available for the modeling period. Major deviations are observed during the exceptionally dry and low stage period in 2001 for the canal (1-8C in Fig. 4) and the adjacent marsh station of 1-8T. As previously noted, this model does not simulate groundwater when observed water levels fall below the marsh surface. As no deficit from below-ground stage conditions needs to be replenished prior to rewetting, the MIKE FLOOD model does tend to recover too quickly from extreme drought. Statistics for the calibration and validation (Tables 3 and 4) of daily water level show that the hydrodynamic model was calibrated well with high correlation coefficients (all above 0.85), low bias (all less than 0.1 m), and high Nash–Sutcliffe efficiency (all above 0.5 except for 1-8C for the validation period).

Comparison of modeled surface water depth with DCS measured during monthly water quality sample collections provided an independent test over a wider spatial extent than was provided by recording stage gages in the marsh (Fig. 5). Monthly water quality samples and DCS are collected in the vicinity of a fixed location. Because they are not taken at exactly the same location each month, DCS measurements are expected to have lower precision than measurements at fixed location stage gages. Furthermore, a positive bias under more shallow conditions was expected because samplers search for a sampling location in the vicinity of the marked sampling site with a minimum 10 cm clear water depth. Despite these complications, the model presented a good fit to the observed variations in DCS at most sites. This further verifies that the model can provide reliable predictions beyond the established stage gage network. It also demonstrates that the effort of carefully measuring DCS during sampling provides valuable data. Observed marsh DCS ranged from a low below 0.1 m typically occurring more in the north, to a high of 0.65 m in the south.

The DCS data provide an independent test of the topographic data used in model development, because at high stage, when there are no large inflows or outflows, the water stage is generally flat across the Refuge. Thus, stage minus DCS provides a good estimate of soil elevation at the sampling site. At the neighboring stations of LOXA130 and LOXA131, it was observed that even though the observed data displayed a similar pattern, the model predic-

Table 3
Calibration statistics of daily water level (2000–2004).

Station	Count (n)	Bias (m)	RMSE (m)	Average observed (m)	Average model (m)	SD observed (m)	SD model (m)	SD error (m)	Variance reduction (%)	R (correl. coef.)	r^2	Nash–Sutcliffe eff.
North	1261	−0.04	0.08	5.10	5.04	0.12	0.14	0.07	62	0.86	0.74	0.51
1-7	1827	−0.01	0.07	5.01	5.00	0.13	0.14	0.06	77	0.89	0.80	0.77
1-8T	1820	0.03	0.08	4.94	4.97	0.20	0.17	0.07	87	0.94	0.89	0.85
1-9	1827	0.00	0.06	4.96	4.97	0.16	0.16	0.06	86	0.94	0.88	0.86
South	1304	0.04	0.07	4.91	4.93	0.21	0.22	0.06	92	0.96	0.93	0.89
1-8C	1827	−0.03	0.09	4.94	4.90	0.28	0.27	0.08	92	0.96	0.92	0.91

Table 4
Validation statistics of daily water level (2005–2006).

Station	Count (n)	Bias (m)	RMSE (m)	Average observed (m)	Average model (m)	SD observed (m)	SD model (m)	SD error (m)	Variance reduction (%)	R (correl. coef.)	r^2	Nash–Sutcliffe eff.
North	725	−0.02	0.04	5.01	4.99	0.09	0.09	0.04	79	0.90	0.80	0.75
1-7	730	−0.03	0.05	4.97	4.95	0.10	0.09	0.05	79	0.89	0.79	0.72
1-8T	694	−0.03	0.07	4.94	4.90	0.14	0.12	0.06	80	0.89	0.80	0.74
1-9	730	−0.04	0.06	4.94	4.91	0.12	0.11	0.05	81	0.90	0.81	0.72
South	704	−0.06	0.09	4.92	4.86	0.15	0.16	0.07	81	0.91	0.84	0.66
1-8C	730	−0.09	0.14	4.94	4.84	0.17	0.21	0.11	57	0.85	0.73	0.24

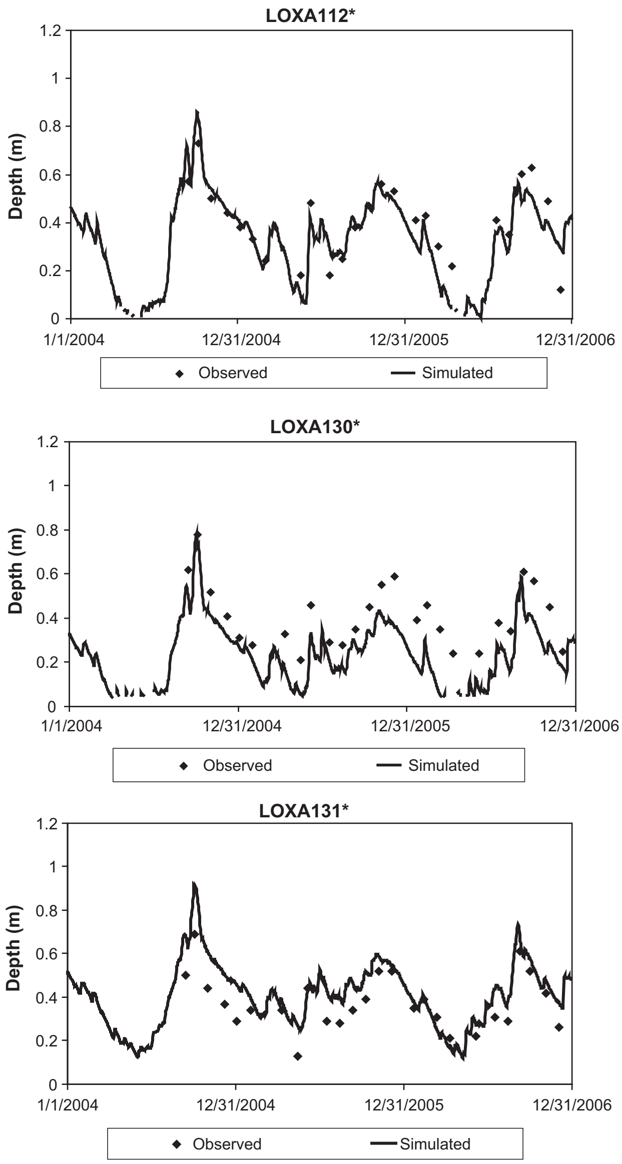

Note: "LOXA" stations are labeled as "A" stations in Figure 3. "*" indicates the observed data for the enhanced stations started from August 2004.

Fig. 5. Comparisons of simulated and observed water depth at selected DCS stations.

tions showed drastically different patterns. Such modeled differences are conjectured to be related to inadequacy of spatial resolution and sampling bias for characterization of topography and vegetation. The influence of local topographic and vegetation features with a scale below the 400 m model resolution may have significant influence on site-specific observations.

6.2. Discharge

The simulated discharges of the four regulatory structures (S-10A, S-10C, S-10D and S-39) were compared with the recorded data. The daily discharge obtained at noon was aggregated to annual discharge. Agreement between the predicted and recorded annual outflows at the four structures combined is not much greater than the uncertainty associated with discharge estimation at gates and pumps (Ansar and Chen, 2009). Statistics of annual discharge over the entire period of simulation for the individual and combined stations (Table 5) demonstrate that the model does predict individual structure flows well, but is more reliable in predicting overall outflow.

6.3. Chloride (Cl) concentration

The modeled chloride concentration was compared with the measured data of the EVPA, XYZ, enhanced water quality network, and the canal hydraulic structure samples for the calibration and validation periods. There are 54 marsh and 11 canal stations. Among those, marsh sampling was typically monthly, but sampling at canal structures was typically irregular. Several representative stations, which broadly cover the Refuge, were selected to illustrate the diversities of chloride concentration over the Refuge (Fig. 6). For those selected stations, the comparison of observed and predicted chloride concentration showed seasonal patterns and instances of high chloride canal water intruding into the peripheral marsh. The occasional gaps in the model results seen in the time series graphs reflected periods where a cell was dry. Gaps in marsh sampling data reflected instances when water was too shallow to sample (i.e., depth of clear water was less than 10 cm). The corresponding statistics for those stations are given in Tables 6 and 7 for the calibration and validation periods, respectively.

The overall model predictions compared well with the observed data for the marsh and the canal stations. The canal station (Z0) and those near the peripheral marsh zones (LOX6 and LOXA117) show greater variation in concentration than the interior station (LOX13). We believe that a major cause of errors in chloride projections can be linked to the low frequency of sampling at the canal inflows. Inflow sampling for chloride was performed by grab sampling approximately every 2 weeks. Chloride concentration was variable and showed some dependence on discharge. Thus, more frequent, or flow proportional sampling was needed to adequately characterize chloride inflow loads; increased sampling frequency or deployment of sondes to log conductivity as a surrogate for chloride concentration at the inflows would address this data need. This improved monitoring would significantly improve model performance. Other sources of uncertainty that impacted the model

Table 5
Statistics of annual discharge of individual outflow structure and combined for the period of 2000–2006.

Station	Count (n)	Bias ($m^3 \times 10^6$)	RMSE ($m^3 \times 10^6$)	Average observed ($m^3 \times 10^6$)	Average model ($m^3 \times 10^6$)	SD observed ($m^3 \times 10^6$)	SD model ($m^3 \times 10^6$)	SD error ($m^3 \times 10^6$)	Variance reduction (%)	R (correl. coef.)	r^2	Nash–Sutcliffe eff.
S-10A	7	8.35	15.59	64.18	72.54	26.92	28.21	14.22	72	0.87	0.75	0.61
S-10C	7	12.83	31.12	59.70	72.54	43.83	28.21	30.63	51	0.72	0.52	0.41
S-10D	7	−4.13	18.01	76.66	72.54	25.06	28.21	18.93	43	0.75	0.57	0.40
S-39	7	7.46	39.31	117.75	125.21	78.66	57.66	41.69	72	0.86	0.73	0.71
S-10ACD	7	17.06	41.59	200.55	217.61	83.69	84.63	40.97	76	0.88	0.78	0.71
S-10ACD+S-39	7	24.51	41.28	318.30	342.81	120.72	102.49	35.87	91	0.96	0.92	0.86

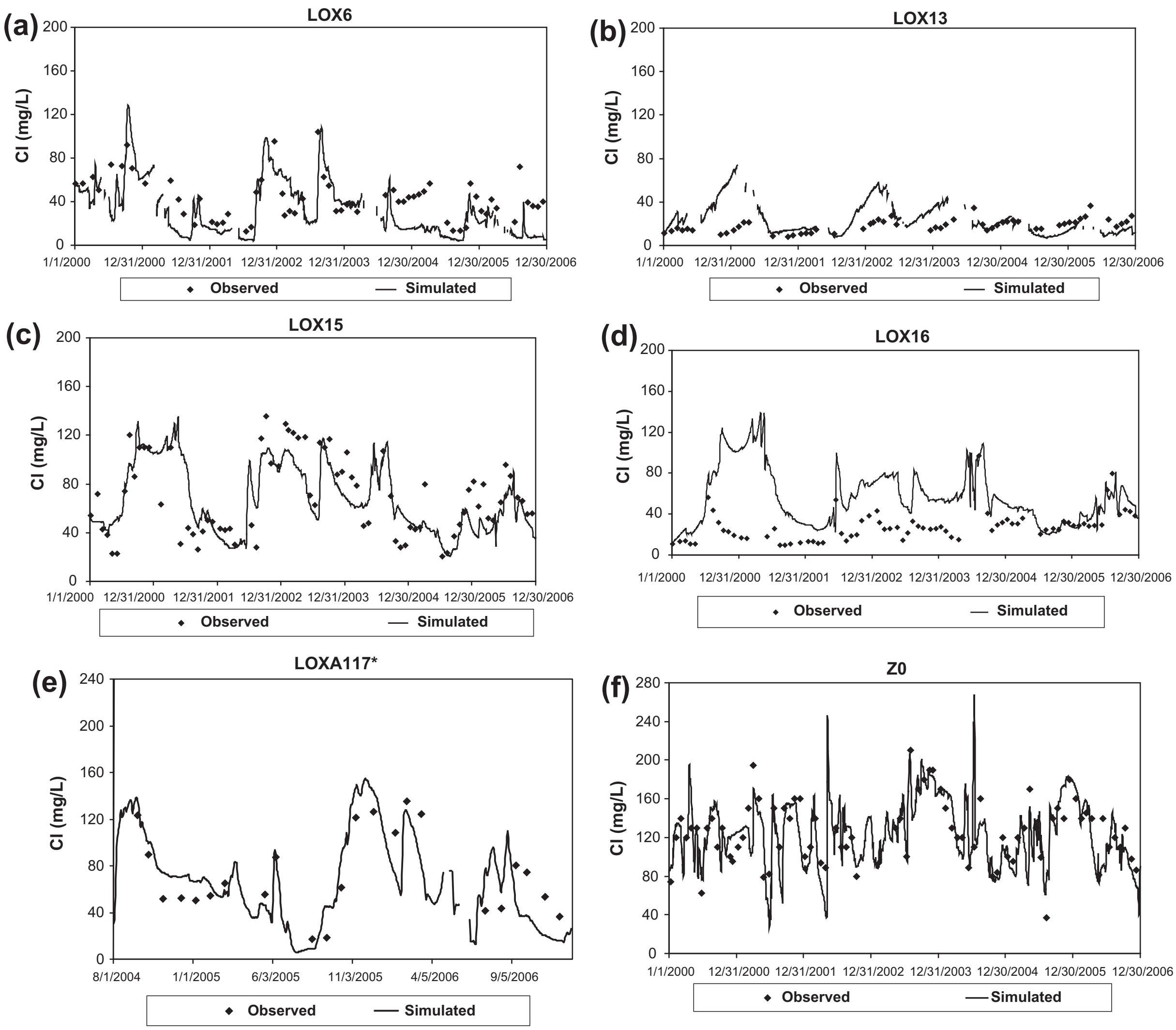

Note: “LOXA” stations are labeled as “A” stations in Figure 3. “*” indicates the observed data for the enhanced stations started from August 2004.

Fig. 6. Comparison of chloride concentration with measured data at selected EVPA (a–d), enhanced (e), and canal (f) stations.

performance include uncertainty in the estimated dry and wet deposition of chloride and the inadequate resolution of topographic data for the Refuge. The few negative Nash–Sutcliff efficiency values indicate that the model does not predict daily values at some Refuge sites with accuracy. We also examined the model’s capability for long term prediction, for which the mean observed concentration was plotted against the mean simulated for the calibration and validation period (Fig. 7). Good agreement was found between these two pairs with the Nash–Sutcliffe efficiency of 0.88 and 0.67 for the calibration and validation, respectively. This indicates that the model did a good job simulating long term chloride variation within the Refuge.

Sampling sites were sorted according to the median of observed chloride concentration, resulting in a list of sites ranging from least-impacted to most-impacted by exogenous mineral impact (Table 8). The seven sites with lowest median values were

Table 6
Statistics of discrete chloride concentration at selected stations for the calibration period (2000–2004).

Station	Count (n)	Bias (mg/L)	RMSE (mg/L)	Average observed (mg/L)	Average model (mg/L)	SD observed (mg/L)	SD model (mg/L)	SD error (mg/L)	Variance reduction (%)	R (correl. coef.)	r^2	Nash–Sutcliffe eff.
LOX6	41	−5.75	25.30	49.63	42.75	25.89	27.15	24.92	7	0.64	0.41	0.08
LOX13	29	14.40	21.60	16.27	29.87	5.64	17.26	16.39	−745	0.31	0.10	−13.78
LOX15	53	1.41	22.59	73.39	74.80	35.36	26.02	22.76	59	0.77	0.59	0.58
LOX16	51	35.85	42.33	24.72	60.57	15.19	25.74	22.73	−124	0.48	0.23	−6.92
Z0	55	0.63	28.34	126.78	127.42	33.48	38.97	28.59	27	0.70	0.49	0.27

Table 7
Statistics of discrete chloride concentration at selected stations for the validation period (2005–2006).

Station	Count (n)	Bias (mg/L)	RMSE (mg/L)	Average observed (mg/L)	Average model (mg/L)	SD observed (mg/L)	SD model (mg/L)	SD error (mg/L)	Variance reduction (%)	R (correl. coef.)	r^2	Nash–Sutcliffe eff.
LOX6	20	−22.78	27.69	37.39	14.58	15.22	8.50	16.16	−13	0.25	0.06	−2.16
LOX13	14	−5.69	7.18	22.11	14.84	4.88	5.51	4.54	13	0.57	0.32	−3.10
LOX15	22	−11.40	17.29	58.58	47.18	19.76	13.53	13.30	55	0.74	0.55	0.20
LOX16	22	5.75	10.94	35.19	40.94	13.40	13.74	9.52	50	0.75	0.57	0.30
Z0	24	−2.07	18.95	122.96	120.89	31.64	32.95	19.24	63	0.82	0.68	0.63
LOXA117[a]	23	−2.94	25.07	70.89	67.95	36.73	39.15	25.58	51	0.77	0.60	0.51

[a] The data for the enhanced stations started from August 2004. The statistics are calculated for the period from the date when the data become available to the end of 2006.

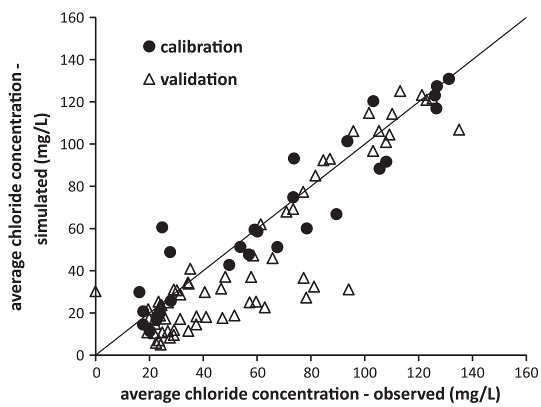

Fig. 7. Scatter plot of mean observed and mean simulated chloride concentration for the calibration period (EVPA, XYZ, and canal stations) and the validation period (EVPA, XYZ, enhanced, and canal stations).

classified as least-impacted with observed median concentration averaged 20.5 mg/L, and ranged from 17.1 to 23.2. These sites tend to be farther from the canal than other sites. Average observed median concentration at the seven most-impacted averaged 89.9 mg/L, and these sites are generally close to the canal. Sites were classified as transition that had median values between the least-impacted and most-impacted. Average observed median concentration at transition sites was 36.3 mg/L. The pattern of a high gradient and highly variable chloride concentration among the most-impacted and transition sites, combined with the low and less-variable chloride concentrations at the least-impacted sites, has, we believe, led other researchers to conclude that the Refuge interior is properly classified as ombrotrophic (McCormick and Crawford, 2006).

The qualitative spatial pattern of observed chloride concentration was reproduced by the model. Calibration and validation simulations were combined into a base run. For comparison with

Table 8
Median values (mg/L) of the observed, base and the scenario simulated chloride concentrations at the least-impacted, transition and most-impacted sites.

Site	Observed	Base	Scenario 1	Scenario 2	Distance from canal (km)
Least-impacted					
LOX13	17.1	18.7	5.3	14	6.6
LOX11	18.6	16.6	5.6	11.2	6.5
LOX3	18.8	14.2	4.1	7.6	4.6
LOX5	20.3	9.0	3.9	6.2	8.1
LOX8	22.8	14.1	4.7	8.2	9.7
LOX9	23.0	21.2	4.9	18.4	5.5
LOX7	23.2	14.3	5.1	8.1	5.5
Average	20.5	15.4	4.8	10.5	6.6
Transition					
LOX14	25.5	37.5	5.6	12.4	1.2
LOX16	26.0	52.5	5.5	44.4	2
LOX10	30.0	39.5	4.5	37.2	1.2
X4	35.0	34	5.0	29.8	4.2
Z4	37.0	36.2	5.1	34.6	3.0
LOX12	38.0	42.0	5.3	37.3	2.7
LOX6	42.4	24.1	4.9	7.3	1.1
Y4	43.0	39.1	4.8	36.2	3.1
X3	50.0	48.6	4.7	47.6	2.0
Average	36.3	39.3	5.0	31.9	2.3
Most-impacted					
Z3	55.3	45.2	4.9	44.4	2.2
LOX4	62.3	31.9	4.3	8.2	1.1
LOX15	65	60.4	5.1	53.4	1.2
X2	97	91.3	4.3	82.5	1
Z2	100	88.2	4.1	83.3	1
Z1	120	110	3.2	106.7	0.2
X1	130	119.2	3	118.7	0.2
Average	89.9	78	4.1	71	1

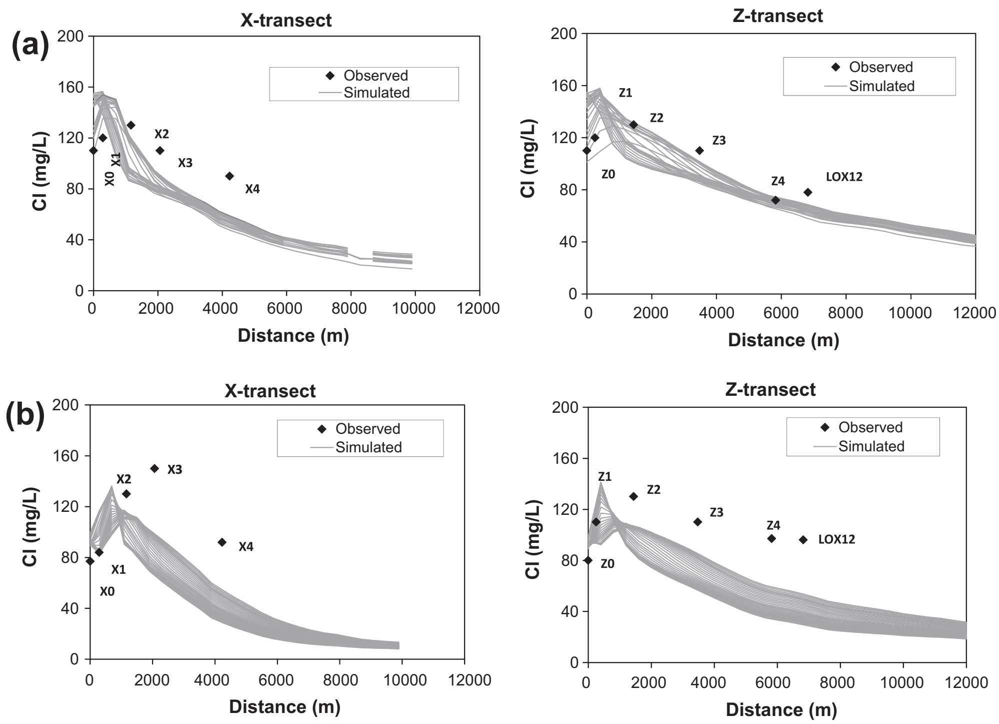

Fig. 8. Chloride concentration of measured and extracted profiles along the X and Z transects with a 2-week window before and after the measurement (a) event of 9/20/2000 (window 9/6/2000–10/4/2000); (b) event of 10/15/2002 (window10/2/2002–10/29/2002).

observed median values, simulated base run values were paired by date (Table 8). Although displaying a similar pattern, modeled base run median values are lower than observed at 18 of the 23 sites evaluated.

To evaluate the impacts of canal water intrusion, concentration profiles along two transects around the XYZ stations were extracted. The X-transect includes stations X0, X1, X2, X3, and X4; and the Z-transect includes stations Z0, Z1, Z2, Z3, Z4, and LOX12. Fig. 8 shows the comparisons of observed concentration and profiles of model results for two intrusion events occurred in 2000 and 2002, respectively. The field measurements used in the profiles were gathered at different times. Therefore, model results were extracted over a time period including the duration over which the field data was gathered. A 4-week window around the field measurements proved sufficient to capture the intrusion event. In general, the concentration gradient pattern was reproduced by the model. The elevated concentration observed from the transitional zone towards the interior marsh indicates that there is substantial canal water intrusion extending a few kilometers into the marsh. The modeled concentration, in general, declines more rapidly along canal–marsh transects than is observed. This may result from inadequate vegetation and topographic data to adequately describe the zone across peripheral marsh to the canal levee.

7. Pumped inflow impact analysis

The calibrated and validated model provides an analysis tool for quantifying projected impacts of proposed structural or operational alternatives. Herein, two scenarios were examined. Scenario 1 quantifies the importance of chloride loading from inflows on Refuge chloride levels (the completely rainfall-driven test scenario), while scenario 2 illustrates the efficacy of a hypothetical project designed to block overbank flow along the eastern canal (the barrier scenario).

7.1. Chloride inflow concentration reduction scenario analysis (scenario 1)

The chloride concentrations at all the inflow structures along the length of the perimeter canal were reduced to a constant 2 mg/L, a value equal to the concentration assumed in wet atmospheric deposition. This modeling experiment examined the influence of the chloride loading from the inflow structures on the marsh interior. The comparison of concentration for the original boundary concentration (referred to herein as the "Base" condition) and the reduced inflow concentration (2 mg/L) provided an estimation and visualization of the flushing time of water in the marsh and canal systems as both models use the same initial concentration (Fig. 9). The flushing time at the selected marsh sites (Fig. 9a and b) was equal to or greater than 1 year, but the canal (Fig. 9c) initially responded much more rapidly, while continued to respond as chloride flows from the marsh.

This scenario also quantified the concentrating of chloride through evaporation (a distillation process) by simulating marsh that is no longer impacted by canal water intrusion. During the dry season, when ET and seepage exceed precipitation, the chloride concentration increased and at times reached as high as 12.5 mg/L for LOX10 and 18.6 mg/L for LOX11. When the wet season started, the rainfall diluted the concentration, but most marsh stations remain over 3 mg/L. Evaporation therefore concentrated chloride at times by a factor of 1.5 to nearly 10 at more isolated interior marsh sites like LOX11. Although the concentrating effect of evaporation does at times significantly raise modeled chloride concentrations, comparison to base run concentrations at these sites illustrate that most of the chloride mass observed at interior sites originates at pumped inflows rather than in aerial deposition.

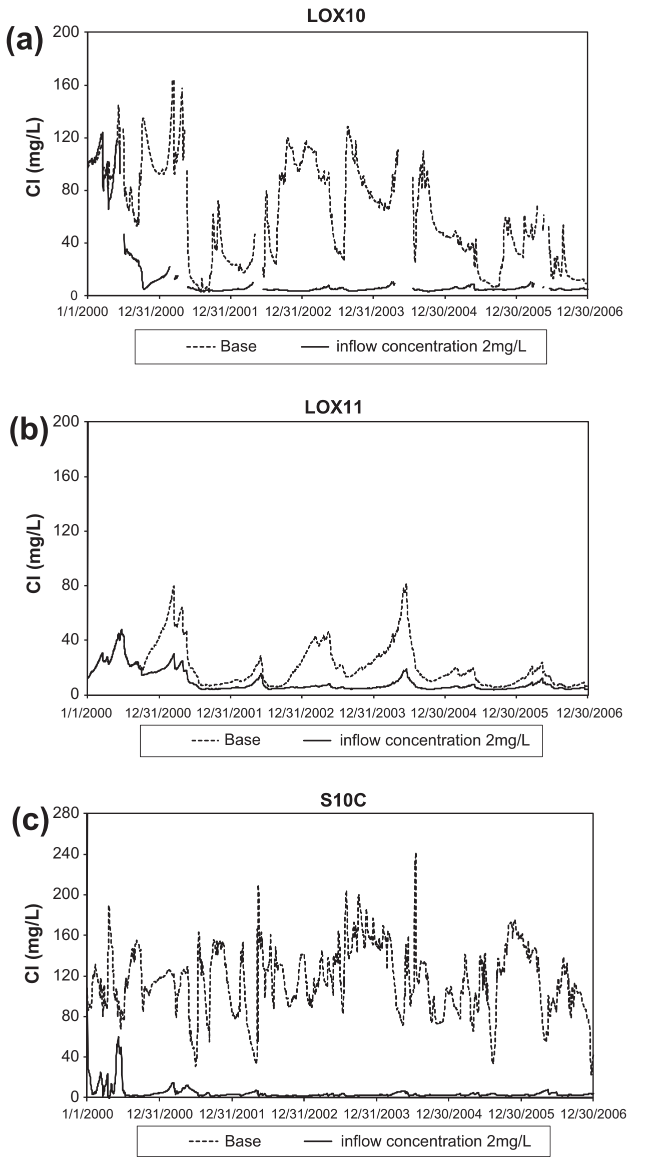

Fig. 9. Comparison of chloride concentration with original boundary inflow concentration (base) and reduced concentration (2 mg/L, same as rainfall concentration) at selected marsh stations (a and b) and canal station (c).

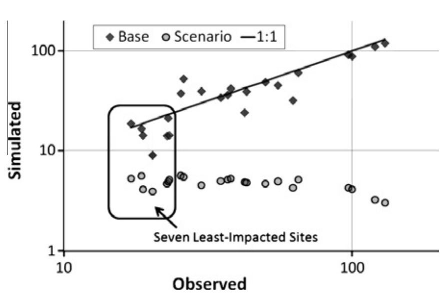

Fig. 10. Scatter plot of median concentration for the base and scenario 1.

Observed chloride grab sample concentrations were paired by date with simulated chloride concentrations. The median values at the EVPA and the XYZ stations for the observed concentrations, base simulation, and the scenario simulation results were calculated (Table 8, Fig. 10). From this list, the seven least-impacted (lowest median chloride concentration) sites, and seven most impacted sites were identified. The average median concentration of the seven least-impacted sites is 15.4 mg/L for the base case, and 4.8 mg/L for the scenario. Thus, chloride concentration in the marsh under the base condition is over three times that of the reduced concentration scenario which indicates that chloride in the marsh primarily comes from the pumped inflows. This shows that the least-impacted marsh is not ombrotrophic and is not properly described as a rainfall-driven system.

7.2. Preliminary analysis of an eastern canal–marsh barrier (scenario 2)

At times, water supply use has been routed through the eastern Refuge L-40 Canal for delivery to users east and southeast of the Refuge. It has been proposed (SFWMD, 2005b) that it would be beneficial to greatly reduce or eliminate contact and mixing between the water from the eastern canal and the marsh because that would reduce marsh nutrient and mineral concentration, and might avoid unnecessarily treating water that is simply being routed to water supply structures. In this scenario, a hypothetical barrier is built along the eastern canal. The barrier was modeled by simply removing the links between the canal and marsh along the entire length of the eastern canal. Comparisons of stage and concentration at several stations between the base conditions (without barrier) and with barrier show little impact on marsh stage, and significant reduction of chloride concentration at some sites (Fig. 11).

The Refuge's WRS primarily uses the stage measured in the eastern (L-40) canal to require regulatory water releases. When pumped inflows discharge into the L-40 canal, a transient local water accumulation and stage rise occurs that may result in additional regulatory discharge. The resultant effect is that the canal water was drained faster, which leads to a slightly lower stage than the base conditions (1-8C, Fig. 11a). Minor operational changes could be used in the future to reduce this excessive regulatory release. The water stage in the easternmost region of the marsh (1-8T, Fig. 11b) increased as rain water could not be drained to the eastern canal.

Blockage of the marsh flow to the eastern canal caused the chloride concentration in the eastern canal to increase (G-94B, Fig. 11g). The effect of constructing the barrier on the western marsh and canal is not as pronounced, but did reduce chloride concentrations. The chloride concentrations decreased slightly in the western canal (X0, Fig. 11f) as well as adjacent western marsh sites (LOX10, Fig. 11c). The decrease demonstrates that additional low chloride runoff from the marsh interior that would have drained to the eastern canal is forced by the barrier to flow to the west.

For the marsh interior the chloride concentration was drastically reduced at eastern sites (LOX14, Fig. 11e) due to the protection from the eastern canal water intrusion events, while only slightly reduced in the western marsh (LOX10, Fig. 11c). Minor decrease was even found for the more isolated interior marsh sites (LOX13, Fig. 11d). Based on our model simulations, we project that with the barrier in place, canal water of higher concentration would be directed south down the eastern canal, and would substantially reduce high concentration canal water from penetrating into the Refuge. This analysis focused on characterizing hydrology and canal–marsh dynamics related to a barrier. It is important to note that no ecological or other analyses were conducted. This analysis demonstrates a potential for a water quality benefit from physically barring water penetration into the marsh, but any management decision to support such an extensive and intrusive structure would require further detailed consideration and design to quantify the multiple direct and indirect wetland impacts and benefits of alternatives.

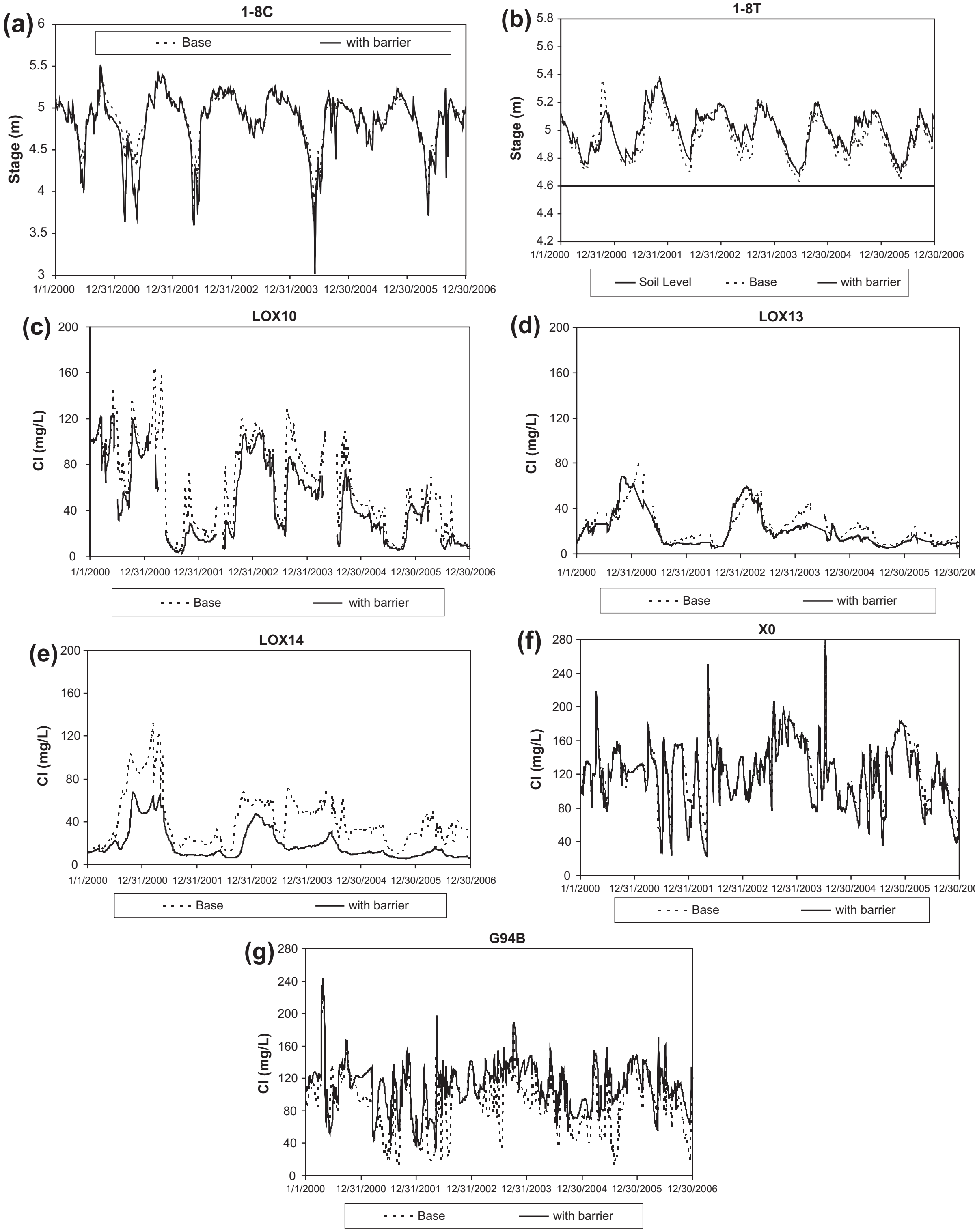

Fig. 11. Comparison of simulated stage (a and b) and chloride concentration (c–g) without barrier (base) and with barrier at selected marsh and canal stations.

8. Discussion

Our study simulated regulatory outflows triggered by stages higher than a seasonally variable regulation schedule, and used historical flows for water supply and storm-forecast related outflows. Thus, our model adjusted regulatory outflow under the barrier scenario to account for altered canal stage. Decisions on regulatory water releases from the Refuge often depend partially on information unavailable within the Refuge model (stages downstream, weather forecasts, and water supply needs), as well as professional judgment of water managers. Any model of regulatory outflow operations is challenging and should be tested before being used in analyses involving changes in Refuge inflows and outflows (Arceneaux et al., 2007). In our approach, historic structure outflow provides an additional calibration test through comparison of modeled outflows with calibration and validation results to test if our stage–discharge relationship is credible.

Calibration shows that stage is relatively insensitive to certain hydrologic parameters, such as canal and marsh roughness, and dry and wet depths. Site-specific velocity and patterns of mass transport, however, are sensitive to these parameters. One could use velocity measurements as added calibration criteria to augment the stage calibration criteria, but such measurements were unavailable in the canal or marsh to apply to model calibration. Indeed, velocity measurements of adequate spatial and temporal resolution are technically challenging and expensive, particularly in the spatially heterogeneous marsh system. Because of the conservative nature of chloride, inclusion of this constituent into the model calibration provides an alternative to identify deficiencies and evaluate the adequacy of model predicted flows.

Chloride was found to be sensitive to both dispersion and roughness, but these parameters had quite different spatial patterns of sensitivity. Chloride was found to be more sensitive to dispersion in the interior marsh than in the peripheral marsh. This can be explained that velocity in the interior is low, and chloride is transported mainly by dispersion compared to the peripheral zone where transport is dominated by advection. Inversely, roughness plays a more important role in the peripheral marsh because of the relatively higher velocities and advective transport.

Literature survey reveals that dispersion in large wetland systems is not well studied. In surface water modeling, the dispersion coefficient can vary over 11 orders of magnitude, ranging from 10^{-5} cm^2/s for molecular diffusion to well over 100 m^2/s for some cases of dispersion in open estuaries (Bowie et al., 1985). In our calibration, it was found that dispersion in the central area of the marsh wetland was best characterized by a dispersion coefficient of 2 m^2/s. Although this is below values typically estimated in open-water, it is more than an order-of-magnitude above the dispersion measured in laboratory flume studies with flow around simulated emergent plant stems (Nepf et al., 1997; Lightbody and Nepf, 2006). This result suggests that dispersion modeled here largely results from the heterogeneity of flow paths and velocities that exist in this natural wetland. It further suggests that stagnant zones (dead zones) and short circuiting along sloughs and boat trails may play a similarly significant role in affecting dispersion in a natural wetland as it does in constructed wetland treatment systems (Martinez and Wise, 2003; Paudel et al., 2010).

The 400 m grid currently employed in the model is the best topographic resolution currently available to the Refuge, but still restrains model performance from fully capturing some events. It does not capture the sloughs or other topographic features that may impact circulation patterns within the marsh interior. Further, available topographic data do not capture microtopographic features that likely control flows at shallow depths. Min and Wise (2009) has demonstrated through simulation models that small scale topographic variation can have a large impact on mixing and dispersion. The importance of local site-specific conditions was illustrated in this study by sampling sites LOX15 and LOX16 (Fig. 6). Although these stations are at a similar distance to the canal and are close to each other, they at times display a considerable divergence in observed chloride concentration. From a modeling perspective, it appears that station LOX16 is somehow isolated from canal water carrying high chloride concentrations by topographic or vegetative features that were not captured in the topographic or vegetation surveys, and thus not properly reflected in the model. As also demonstrated by the discrepancy in modeled water depth for geographically close stations of LOXA130 and LOXA131 (Fig. 5), it is believed that certain areas in the marsh interior are more protected or exposed by local features. As with all models, this model must be interpreted with an understanding of the uncertainty introduced by local topography and other local conditions beyond the resolution of the model input data.

Our modeling has shown that MIKE FLOOD is an efficient tool for simulating the hydrodynamics and constituent transport between canal and marsh. It takes approximately 70 min to run a year of simulation on 2.83 GHz Intel(R) Core(TM)2 Quad CPU. However, several limitations were identified for this model. Bed roughness was found to be essential for proper modeling of chloride transport. However, MIKE 21 does not include the capability to define depth-dependent roughness, thus the resistance of the marsh was defined based on vegetation. As no ET or groundwater model was included, the ET reduction and seepage rate were imposed and calibrated. Finally, as needed by the commercial proprietary software license, the MIKE FLOOD model is not easily portable and accessible to other interested agencies or researchers.

9. Conclusions

In this paper, we demonstrated that the MIKE FLOOD program provides a useful platform for simulation of the hydrology of a large coupled canal and marsh system. It dynamically couples a 1-dimensional channel model and a 2-dimensional structured-grid overland flow model. The user programmable ECO Lab module provides a practical tool for constituent simulation, and provides considerably greater flexibility of model structure definition when compared to solely using the advection–dispersion module available in MIKE FLOOD. The graphical and statistical analysis of the model performance using observed water levels, water depths, discharge, and chloride concentrations demonstrates that this model typically provides good long-term projections of the Refuge hydrodynamics and chloride concentration that result from inflows and outflows over long and short temporal scales. It is essential for the Refuge to have the capability of assessing and comparing alternative water management plans and alternative structures' operation schemes. The calibrated and validated model provides this capability. Additionally, a better understanding of the hydrologic and water quality processes affecting the Refuge and alternative operations of flow structures can be gained through application of hypothetical scenarios.

The model was calibrated to the spatial and temporal patterns of chloride as a conservative constituent. This process assisted in fine tuning the hydrodynamic calibration of water flow. The model also provides a calibrated modeling base for further development of reactive constituents such as total phosphorus and sulfate. Although some specific data limitations were identified with regard to the quality of input data, the Refuge is data-rich and has potential for use as a prototypical system for the testing and development of future wetland models.

The model provides a useful tool for better understanding the causes of canal water intrusion into the marsh, and supplements analyses based solely on monitoring (Harwell et al., 2008; Surratt et al., 2008). Previous applications of MIKE FLOOD focused on rivers, lakes, and estuaries (Patro et al., 2009; Miller and Meselhe, 2008). To the authors' knowledge, modeling a spatially expansive wetland using MIKE FLOOD presented here is unique. As the MIKE FLOOD model structure is capable of simulating large-scale coupled stream-wetland systems, it provides a spatial and temporal resolution that is adequate to credibly support many Refuge management decisions concerning water quality and quantity.

Applications presented here illustrate the value of modeling to contribute to both the understanding of large wetland ecosystems, as well as management of those systems. The interior marsh of the Refuge has often been termed ombrotrophic or rainfall-driven, implying that interior water chemistry is not significantly impacted by the pumped stormwater which discharges into the canals. Using modeling, it was shown here that even at relatively isolated interior sites (e.g., LOX11), chloride primarily originates in pumped inflows rather than rainfall, and therefore no part of the system is appropriately classed as ombrotrophic.

Even when using well-tested software, it is important to test simple mass and volume balance in model output. We found mass balance anomalies in some options including lateral links between the MIKE 11 and MIKE 21 models, and in one complex structure definition. Our preliminary Refuge model used lateral links to couple the MIKE 11 canal model with the MIKE 21 model of the marsh. It simulated stage and discharge well, and tests showed the model conserved water volume. However, mass balance analysis of chloride demonstrated that MIKE FLOOD lateral links (at the time of writing this manuscript) do not adequately conserve constituent mass. Our revised model, which is presented herein, uses standard links to simulate exchange between the MIKE 21 marsh model and the MIKE 11 canal model. The revised model adequately conserves water and mass. However, mass balance error is detectable; this error results from the MIKE 21 implementation of modeling drying and wetting cycles. This error is directly associated with the wet/dry switching frequency and the number of cells involved in the switches. Therefore, modelers are advised to use caution and test mass balance when simulating periods when the cells are cycling between wet and dry states.

We conclude that this model can provide a valuable management tool supporting alternative analysis and operational decisions within the Refuge. An analogous approach toward model development and application should similarly prove to be of value in management of other Everglades wetlands, and in similar large wetland systems.

Acknowledgements

Funds for this project were provided, in part, by the U.S. Department of the Interior, U.S. Fish and Wildlife Service. We thank USGS and the SFWMD for providing stage, flow and water quality data. The work reported in this paper was presented at open, interagency modeling workshops and reviewed by a technical advisory panel: Drs. Vincent Neary (chair), Malcolm L. Spaulding, and John A. McCorquodale. The authors thank Alonso Griborio (Hazen and Sawyer), Hongqing Wang (USGS), Matt Harwell (U.S. Environmental Protection Agency, formerly with USFWS), Robert Kadlec, and William Walker for their helpful comments on the research and manuscript. The findings and conclusions in this paper are those of the authors and do not necessarily represent the views of the U.S. Fish and Wildlife Service.

References

Alvord, H.H., Kadlec, R.H., 1996. Atrazine fate and transport in the Des Plaines wetlands. Ecol. Model. 90 (1), 97–107.

Andersen, J., Refsgaard, J.C., Jensen, K.H., 2001. Distributed hydrological modeling of the Senegal River basin – model construction and validation. J. Hydrol. 247, 200–214.

Ansar, M., Chen, Z., 2009. Generalized flow rating equations at prototype gated spillways. J. Hydraul. Eng. 135 (7), 602–608.

Arceneaux, J., Meselhe, E.A., Griborio, A., Waldon, M.G., 2007. The Arthur R. Marshall Loxahatchee National Wildlife Refuge Water Budget and Water Quality Models. Report No. LOXA07-004, University of Louisiana at Lafayette in cooperation with the U.S. Fish and Wildlife Service, Lafayette, LA. <http://loxmodel.mwaldon.com>.

Berry, D.A., Lindgren, B.W., 1996. Statistics: Theory and Methods. Duxbury Press, New York.

Bowie, G.L., Mills, W.B., Porcella, C.B., Campbell, C.L., Pagenkopf, J.R., Rupp, G.L., Johnson, K.M., Chan, P.W.H., Gherini, S.A., 1985. Rates, Constants, and Kinetic Formulations in Water Quality Modeling, second ed. EPA/600/3-85/040, USEPA Environmental Research Lab, Athens, GA.

Brandt, L.A., 2006. Benefits Anticipated from the 1995 Water Regulation Schedule for Water Conservation Area 1: Review and Analysis. Report No. LOXA06-006. U.S. Fish and Wildlife Service, Boynton Beach, FL. <http://sofia.usgs.gov/publications/reports/wca1_review/>.

Brandt, L.A., Portier, K.M., Kitchens, W.M., 2000. Patterns of change in tree islands in Arthur R. Marshall Loxahatchee. Wetlands 20 (1), 1–14.

Browder, J.A., Gleason, P.J., Swift, D.R., 1991. Periphyton in the Everglades: spatial variation, environmental correlates, and ecological implications. In: Davis, S.M., Ogden, J.C. (Eds.). Proceedings of Everglades Symposium, Key Largo, FL 1989, 76pp. <http://mwaldon.com/Loxahatchee/GrayLiterature/Browder-et-al-1991.pdf>.

Browder, J.A., Gleason, P.J., Swift, D.R., 1994. Periphyton in the Everglades: spatial variation, environmental correlates, and ecological implications. In: Davis, S.M., Ogden, J.C. (Eds.), Everglades: The Ecosystem and its Restoration. St. Lucie Press, Boca Raton, FL, pp. 79–418 (Chapter 16).

Charman, D., 2002. Peatlands and Environmental Change. John Wiley and Sons Ltd., West Sussex, England, 301 p.

Chen, C., Meselhe, E.A., Waldon, M.G., Griborio, A., Wang, H., Harwell, M.C., 2010. Spatially Explicit Modeling of Hydrodynamics and Constituent Transport within the A.R.M. Loxahatchee National Wildlife Refuge, Northern Everglades, Florida. Report No. LOXA10-003, University of Louisiana – Lafayette in Cooperation with the U.S. Fish and Wildlife Service, Lafayette, LA. <http://sofia.usgs.gov/lox_monitor_model/reports/>.

Daroub, S., Stuck, J.D., Rice, R.W., Lang, T.A., Diaz, O.A., 2002. Implementation and Verification of BMPs for Reducing P Loading in the EAA and Everglades Agricultural Area BMPs for Reducing Particulate Phosphorus Transport. Phase 10 Annual Report. WM 754, Everglades Research and Education Center, Institute of Food and Agricultural Sciences, University of Florida, Belle Glade, FL.

Desmond, G., 2003. South Florida High-accuracy Elevation Data Collection Project. FS-162-96, U.S. Department of the Interior, U.S. Geological Survey, Reston, VA. <http://sofia.usgs.gov/publications/fs/162-96/>.

DHI Water & Environment, 2008. MIKE 21 FLOW MODEL, Advectio/Dispersion Module: User Guide. Hørsholm, Denmark. <http://www.dhigroup.com/>.

Gilvear, D.J., Bradley, C., 2000. Hydrological monitoring and surveillance for wetland conservation and management; a UK perspective. Phys. Chem. Earth (B) 25 (7–8), 571–588.

Harwell, M.C., Surratt, D.D., Barone, D.M., Aumen, N.G., 2008. Conductivity as a tracer of agricultural and urban runoff to delineate water quality impacts in the northern Everglades. Environ. Monit. Assess. 147, 445–462.

Hollis, G.E., Thompson, J.R., 1998. Hydrological data for wetland management. J. Charter. Inst. Water Environ. Manage. 12, 9–17.

Kadlec, R.H., Hammer, D.E., 1988. Modeling nutrient behavior in wetlands. Ecol. Model. 40, 37–66.

Kadlec, R.H., Knight, R.L., 1996. Treatment Wetlands. CRC Lewis Publishers, Boca Raton, FL, 934 pp.

Koskiaho, J., 2003. Flow velocity retardation and sediment retention in two constructed wetland-ponds. Ecol. Eng. 19 (5), 325–337.

Lightbody, A.F., Nepf, H.M., 2006. Prediction of velocity profiles and longitudinal dispersion in emergent salt marsh vegetation. Limnol. Oceanogr. 51 (1), 218–228.

Martin, J.F., Reddy, K.R., 1991. Modeling nutrient retention of freshwater coastal wetland: estimating the roles of primary productivity sedimentation, resuspension, and hydrology. Ecol. Model. 54, 151–187.

Martinez, C.J., Wise, W.R., 2003. Hydraulic analysis of Orlando easterly wetland. J. Environ. Eng. 129 (6), 553–560.

McCormick, P., Crawford, E.S., 2006. Vegetation Responses to Mineral Gradients in an Ombrotrophic Northern Everglades peatland, the Arthur R. Marshall Loxahatchee National Wildlife Refuge. Greater Everglades Ecosystem Restoration Conference, Orlando, FL.

Meselhe, E.A., Griborio, A., Gautam, S., 2005. Hydrodynamic and Water Quality Modeling of the A.R.M. Loxahatchee National Wildlife Refuge – Phase 1: Preparation of Data – Data Acquisition and Processing. University of Louisiana at Lafayette, Lafayette, LA, 248 pp.

Meselhe, E.A., Arceneaux, J.C., Waldon, M.G., 2010. Water budget model for a remnant northern Everglades wetland. J. Hydraul. Res. 48 (1), 100–105.

Miller, R., Meselhe, E.A., 2008. Louisiana Chenier plain regional hydrodynamic and salinity numerical model. In: Proceedings of the Tenth International Conference on Estuarine and Coastal Modeling Congress, 2007, pp. 407–426.

Min, J.H., Wise, W.R., 2009. Simulating short-circuiting flow in a constructed wetland: the implications of bathymetry and vegetation effects. Hydrol. Process 23 (6), 830–841.

Nash, J.E., Sutcliffe, J.V., 1970. River flow forecasting through conceptual models. Part I – A discussion of principles. J. Hydrol. 10 (3), 282–290.

Nepf, H.M., Mugnier, C.G., Zavistoski, R.A., 1997. The effects of vegetation on longitudinal dispersion. Estuar. Coast. Shelf Sci. 44 (6), 675–684.

Newman, S., Reddy, K.R., DeBusk, W.F., Wang, G.S., Fischer, M.M., 1997. Spatial distribution of soil nutrients in a northern Everglades marsh: water conservation area 1. Soil Sci. Soc. Am. 61 (4), 1275–1283.

Patro, S., Chatterjee, C., Mohanty, S., Singh, R., Raghuwanshi, N.S., 2009. Flood inundation modeling using MIKE FLOOD and remote sensing data. J. Indian Soc. Remote Sens. 37 (1), 107–118.

Paudel, R., Min, J.H., Jawitz, J.W., 2010. Management scenario evaluation for a large treatment wetland using a spatio-temporal phosphorus transport and cycling model. Ecol. Eng. 36 (12), 1627–1638.

Richardson, J.R., Bryant, W.L., Kitchens, W.M., Mattson, J.E., Pope, K.R., 1990. An Evaluation of Refuge Habitats and Relationships to Water Quality, Quantity, and

Hydroperiod: a Synthesis Report. Florida Cooperative Fish and Wildlife Research Unit, University of Florida, Gainesville.

Roth, B.W., 2009. Modeling Hydrodynamics and Water Quality in the Arthur R. Marshall Loxahatchee National Wildlife Refuge. Master Thesis, University of Louisiana at Lafayette.

SFWMD, 2005a. Documentation of the South Florida Water Management Model Version 5.5. South Florida Water Management District, West Palm Beach, FL.

SFWMD, 2005b. Conceptual Plan for Preserving the Soft Water Rainfall-based Ecosystem of the A.R.M. Loxahatchee National Wildlife Refuge. South Florida Water Management District, West Palm Beach, FL.

SFWMM, 2000. Florida Land Use and Cover Classification System (FLUCCS).

Surratt, D.D., Waldon, M.G., Harwell, M.C., Aumen, N.G., 2008. Time-series and spatial tracking of polluted canal water intrusion into wetlands of a national wildlife refuge in Florida, USA. Wetlands 28 (1), 176–183.

Swift, D.R., 1981. Preliminary Investigations of Periphyton and Water Quality Relationships in the Everglades Water Conservation Areas: February 1978–August 1979. DRE-131, South Florida Water Management District, West Palm Beach, FL.

Swift, D.R., 1984. Periphyton and water quality relationships in the Everglades water conservation areas. In: Gleasoned, P.J. (Ed.), Environments of South Florida Present and Past II. Miami Geological Society, Coral Gables, FL, pp. 97–117. <http://mwaldon.com/Loxahatchee/GrayLiterature/Swift-1984.PDF>.

Swift, D.R., Nicholas, R.B., 1987. Periphyton and Water Quality Relationships in the Everglades Water Conservation Areas: 1978–1982. DRE-233, South Florida Water Management District, West Palm Beach, FL. <http://mwaldon.com/Loxahatchee/GrayLiterature/Swift-1987.pdf>.

Tsanis, I.K., Prescott, K.L., Shen, H., 1998. Modeling of phosphorus and suspended solids in Cootes Paradise marsh. Ecol. Model. 114, 1–17.

USACE, 1994. Environmental assessment: modification of the Regulation Schedule Water Conservation Area No. 1. U.S. Army Corps of Engineers, Jacksonville, FL. <http://mwaldon.com/Loxahatchee/GrayLiterature/USACE-1995-Lox-Regulation-Schedule.pdf>.

USFWS, 2000. Arthur R. Marshall Loxahatchee National Wildlife Refuge Comprehensive Conservation Plan. U.S. Fish and Wildlife Service, Boynton Beach, Florida. <http://loxahatchee.fws.gov>.

USFWS, 2007. A.R.M. Loxahatchee National Wildlife Refuge – Enhanced Monitoring and Modeling Program – 2nd Annual Report. Report No. LOXA06-008. U.S. Fish and Wildlife Service, Boynton Beach, FL. <http://sofia.usgs.gov/lox_monitor_model/reports/>.

Wang, H., Meselhe, E.A., Waldon, M.G., Surratt, D., Abdou, S., Chen, C., Harwell, M.C., 2008. Compartment delineation for a wetland water quality model in the northern Everglades, Florida, USA. J. Environ. Hydrol. 16, 36.

Wang, H., Waldon, M.G., Meselhe, E.A., Arceneaux, J.C., Chen, C., Harwell, M.C., 2009. Surface water sulfate dynamics in the northern Florida Everglades, USA. J. Environ. Qual. 38, 734–741.

Zhang, Y., Li, C., Trettin, C.C., Li, H., Sun, G., 2002. An integrated model of soil, hydrology, and vegetation for carbon dynamics in wetland ecosystems. Global Biogeochem. Cycles 16 (4), 1–17.